

Supporting Information

Highly Efficient Bifunctional Nanofiber Catalysts with 3D Hierarchical Nanostructures as Building Blocks for Rechargeable Zn-Air Batteries

Yao Guo,^{a,b} Xueting Zhao,^{a,b} Junheng Huang,^b Ximeng Yin,^b Kai Chen,^b Xiang Hu,^b Yangjie Liu,^b Zhenhai Wen^{b,*}

a College of Chemistry Fuzhou University Fuzhou, Fujian 350002, China

b CAS Key Laboratory of Design and Assembly of Functional Nanostructures, and Fujian Provincial Key Laboratory of Materials and Techniques toward Hydrogen Energy, Fujian Institute of Research on the Structure of Matter, Chinese Academy of Sciences, Fuzhou, Fujian, 350002, China.

E-mail: wen@fjirsm.ac.cn

Experimental Section

Chemicals:

Zinc acetate dihydrate ($\text{Zn}(\text{Ac})_2 \cdot 2\text{H}_2\text{O}$), melamine ($\text{C}_3\text{H}_6\text{N}_6$), N,N Dimethylformamide (DMF), and hexadecyl trimethyl ammonium bromide (CTAB) was purchased from Sinopharm Chemical Reagent Co., Ltd. Ruthenium (IV) oxide (RuO_2), 2-methylimidazole (2MI, $\text{C}_4\text{H}_6\text{N}_2$), potassium hydroxide (KOH), Polyacrylonitrile (PAN, $M_w = 150,000 \text{ g mol}^{-1}$), and cobalt (II) nitrate hexahydrate ($\text{Co}(\text{NO}_3)_2 \cdot 6\text{H}_2\text{O}$) were purchased from Shanghai Macklin Biochemical Co., Ltd. Pt/C (20 wt%) was purchased from Sigma-Aldrich, and Nafion D-521 dispersion (5% w/w in water and 1-propanol, $\geq 0.92 \text{ meq/g}$ exchange capacity) was purchased from Alfa Aesar. All reagents were analytical grade and used as received without further purification.

Synthesis of ZIF-8 precursor

Typically, 9.2 mg of CTAB and 11.2 g of 2-MI were dissolved in 50 mL of water and stirred for 15 minutes to form a homogeneous solution. 3 g of $\text{Zn}(\text{Ac})_2 \cdot 2\text{H}_2\text{O}$ was dissolved in 50 mL of water. The two solutions were rapidly mixed, the resulting suspension turned white after 20 s and aged for 3 h at room temperature. The white powder was obtained by centrifugation at 10,000 rpm for 25 min, washed with deionized water and dried at 60 °C for 24 h.¹

Synthesis of CoCNTs/PCNFs and Co/PCNFs

First, 0.5 g of the ZIF-8 was dissolved in 5.0 g DMF and stirred for 2 h, followed by the addition of 0.6 g PAN with stirring for 12 h to yield a milky precursor solution for electrospinning. Then, the precursor solution was placed in a 5 mL syringe with a stainlesssteel needle (1.80 mm in diameter). When electrospinning, the applied voltage was 21 kV, the solution feed rate was 0.6 mL h^{-1} , and the distance between the spinneret and collector was 25 cm. The obtained white ZIF-8@PAN nanofibers mat was divided into small pieces with a size of $4 \times 10 \text{ cm}^2$. Typically, 0.146 g of $\text{Co}(\text{NO}_3)_2 \cdot 6\text{H}_2\text{O}$ was dissolved in 10 mL of deionized water (DI) as solution A, 0.329 g of 2-MI was also dispersed in 10 mL of DI as solution B, then the A solution was quickly added into the B solution and stirring for 25 s to form purple solution. The prepared $10 \times 10 \text{ cm}^2$ ZIF-8@PAN nanofibers mat was directly immersed in the solution and aged for 1 h at room

temperature, then washed with DI and dried under vacuum oven at 70 °C. The obtained purple ZIF-8@PAN membrane coating with ZIF-67 was named as ZIF-67/ZIF-8@PAN. The ZIF-67/ZIF-8@PAN nanofibers film and melamine were heated at a ramping rate 1 °C·min⁻¹ to 250 °C and keep for 5 h, then carbonized for 3 h with a heating rate of 3 °C·min⁻¹ to a certain temperature (600, 700, 800, 900 °C) under Ar/H₂ (10%) atmosphere. The different carbonation temperature cobalt-anchored carbon nanotubes/porous carbon nanofibers (CoCNTs/PCNFs-*T*) were obtained (*T* represents the carbonization temperature). The Co/PCNFs was synthesized without the addition of C₃H₆N₆.

Synthesis of CNFs and PCNFs

Typically, 0.5 g PAN was slowly added to 5.0 g DMF and stirred for 12 h at room temperature to form a yellow precursor solution for electrospinning. The obtained white PAN nanofibers mat was obtained by the same electrospinning treatment, then carbonized at 800 °C to obtain carbon nanofibers (CNFs). The prepared ZIF-8@PAN was directly carbonized to obtain porous carbon nanofibers (PCNFs).

Characterizations: X-ray powder diffraction (XRD) patterns were recorded by Miniflex600 powder X-ray diffractometer using nickel-filtered Cu K α radiation. The morphology and structure of the samples were analyzed by scanning electron microscopy (SEM, Zeiss-Sigma 300), transmission emission electron microscopy (TEM, FEI F20), and HRTEM and Energy dispersive X-ray (EDX) spectroscopy experiments. The chemical state of elements was investigated by X-ray photoelectron spectra (XPS, ESCALAB 250). The Raman spectra were obtained by a Renishaw in Via Raman Microscope (532). Specific surface area and pore size distribution of the samples was examined by the Brunauer-Emmett-Teller (BET) method using nitrogen adsorption and desorption isotherms on a Micromeritics Instrument Corporation sorption analyzer (Micromeritics TriStar II 3020).

Electrochemical measurements

All electrochemical measurements were conducted in a electrochemical workstation employing a standard three-electrode system (CHI 760E, Shanghai Chenhua, China). In this workstation, the carbon rod and Hg/HgO (1.0 M KOH solution) were applied as

the counter and reference electrodes, respectively. To prepare the ink of the working electrode, 5.0 mg of as-prepared catalyst or 20 wt% Pt/C catalyst were dissolved in a mixed solution (including 50 μL of 5% Nafion solution, 475 μL of ethanol, and 475 μL DI water) to obtain a homogeneous catalyst ink under sonicating for 1 h. All measured potentials were referenced to the reversible hydrogen electrode (RHE) using the following Nernst equation.²⁻³

$$E_{RHE} = E_{\text{Hg}/\text{HgO}} + 0.0591 \times \text{pH} + 0.098$$

For the ORR experiment, 8 μL of the catalyst ink was put on the surface of glassy carbon rotating disk electrode (RDE, 3.0 mm in diameter) and dried at room temperature (loading of active materials 0.5 mg cm^{-2}). The cyclic voltammetry (CV) was obtained at a scan rate of 50 mV s^{-1} and the linear sweep voltammetry (LSV) tests was performed with a sweep rate of 5 mV s^{-1} . The electron transfer number (n) can be calculated from the K-L equation.

$$\frac{1}{j} = \frac{1}{j_L} + \frac{1}{j_K} = \frac{1}{B\omega^{1/2}} + \frac{1}{j_K}$$

(1)

$$B = 0.62nF C_{\text{o}_2} D^{2/3} \omega^{1/6} V^{-1/6} \quad (2)$$

$$j_K = nF C_{\text{o}_2} \quad (3)$$

For the RRDE (5 mm in diameter) measurements, the hydrogen peroxide yield (y_{peroxide}) and the electron transfer number (n) can be calculated by the following equations.

$$n = \frac{4NI_d}{NI_d + I_r} \quad (4)$$

$$y_{\text{peroxide}} = \frac{200I_r}{NI_d + I_r} \quad (5)$$

where j is the measured current density, j_K and j_L are the kinetic and limiting current densities, respectively. ω is the electrode rotation speed, F is the Faradaic constant (96,485 C mol⁻¹), C_{O_2} (1.2×10^{-6} mol cm⁻³) and D_{O_2} (1.90×10^{-5} cm² s⁻¹) are the concentration (solubility) and diffusion coefficient of O₂ in 0.1 M KOH, ν is the kinematic viscosity of the 0.1 M KOH solution (0.01 cm² s⁻¹), k is the electron transfer rate constant, and N is the current collection efficiency of RRDE ($N=0.4$), I_r and I_d are the ring current, and the disk current, respectively.

For the OER test of catalyst, 100 μ L ink was put on carbon paper (1×1 cm²) as working electrode, measuring by a conventional three electrode at a scan rate of 5 mV s⁻¹ in 1.0 M KOH. The CV curves were measured at scan rates of 5, 10, 15, 20, 25, 30, 35 and 40 mV s⁻¹, separately.

The ORR stability test was conducted at a constant potential of 0.85 V under a rotating speed (1600 rpm), and the OER stability was performed at potential of 1.56 V. The electrochemical impedance spectroscopy (EIS) measurements for ORR and OER were tested from 100 kHz to 100 mHz at the voltage of 0.85 V and 1.56 V, respectively.

The rechargeable Zn-air battery was tested on home-assembled electrochemical cells, 10 mg prepared catalyst was put on a carbon paper with an area of 1.0 cm² to obtain the air electrode, polished Zn foil was used as anode in 6.0 M KOH mixed with 0.2 M zinc acetate. The area of zinc sheet is 1×3 cm², and the distance between anode and cathode is 0.6 cm. For comparison, 10 mg of mixed powder of 20 wt% Pt/C and RuO₂ with the mass ratio of 1:1 were used to prepare air electrode. The performance of Zn-air battery was measured on a CHI 760E electrochemical workstation. The specific capacity was calculated according to the equation.

$$C = \frac{Q}{\Delta m} = \frac{It}{\Delta m} \quad (8)$$

Where I is the applied current (mA), t is service time (h), and Δm represents the mass of consumed zinc (g).

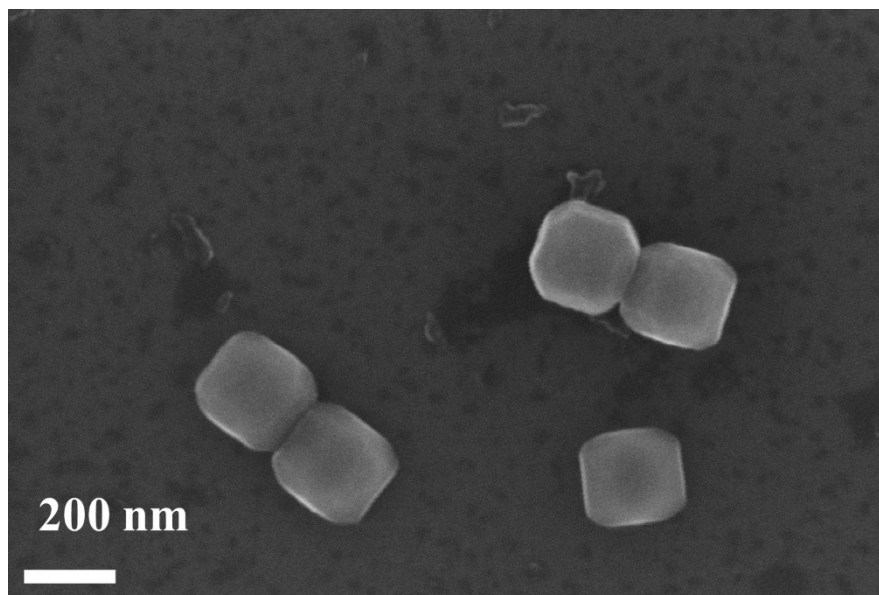


Figure S1. The SEM image of ZIF-8.

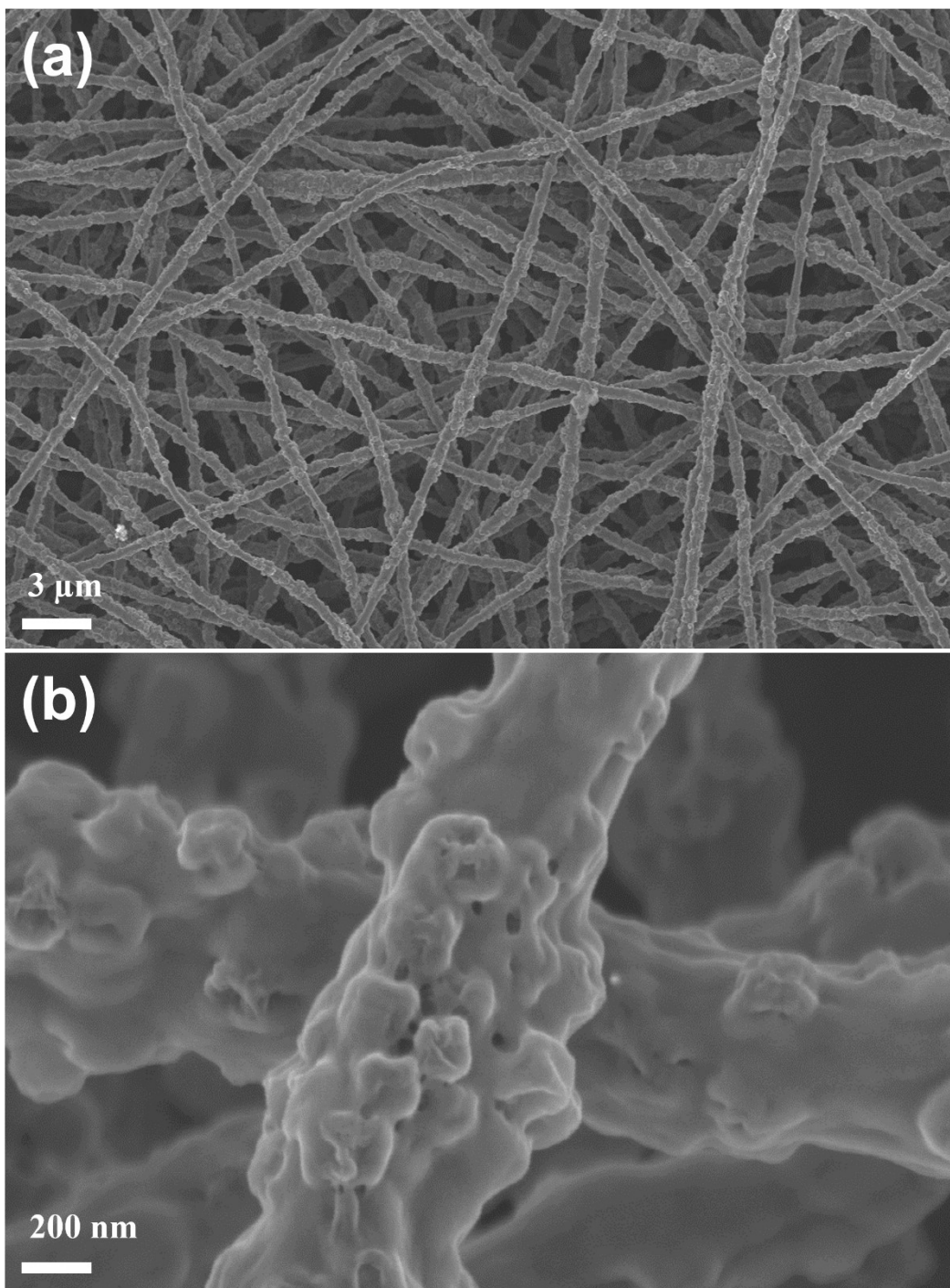


Figure S2. The SEM images of ZIF-8@PAN.

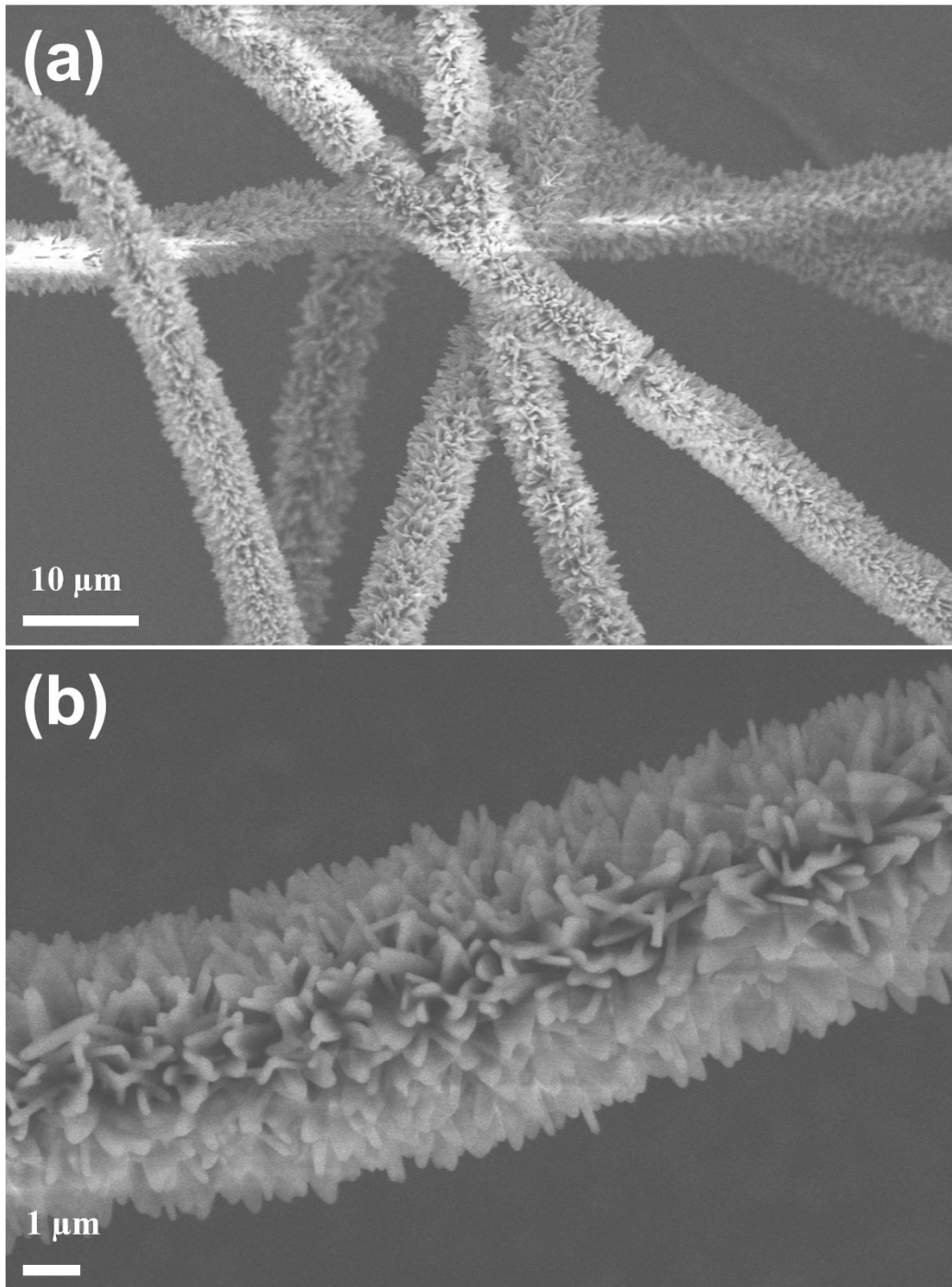


Figure S3. The SEM images of ZIF-67/ZIF-8@PAN.

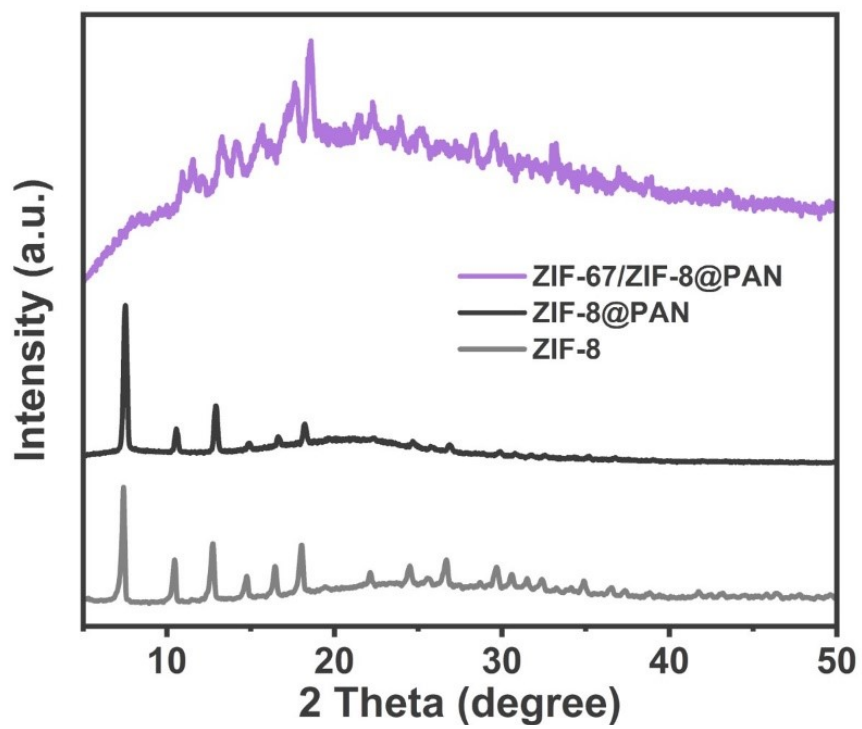


Figure S4. The XRD patterns of ZIF-8, ZIF-8@PAN and ZIF-67/ZIF-8@PAN.

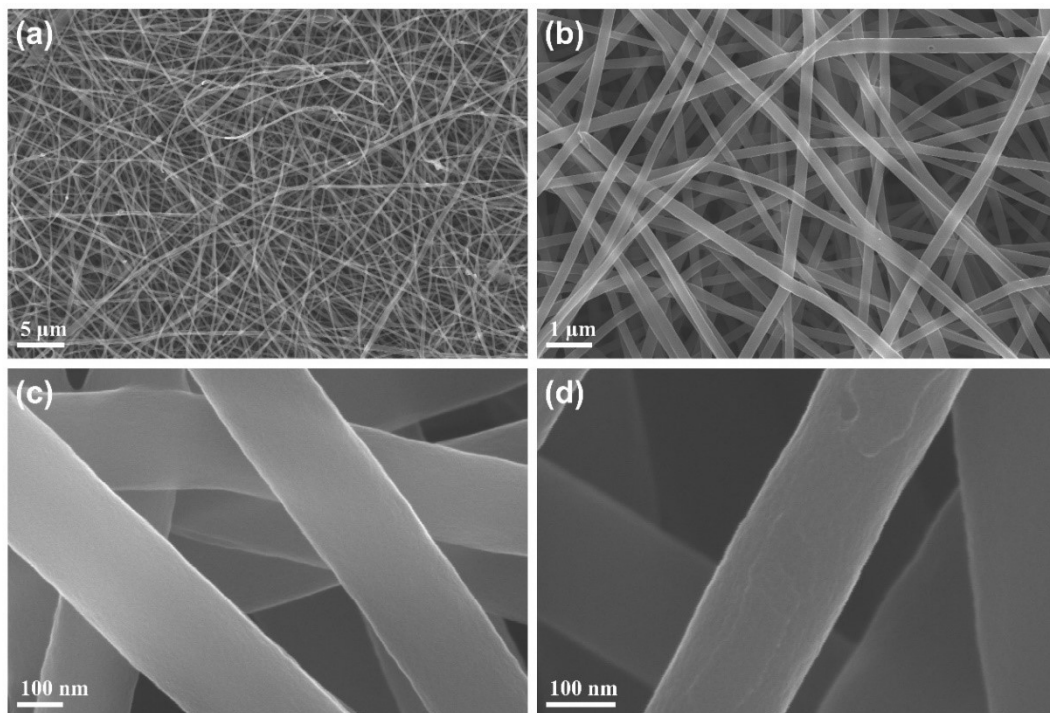


Figure S5. The SEM images of CNFs.

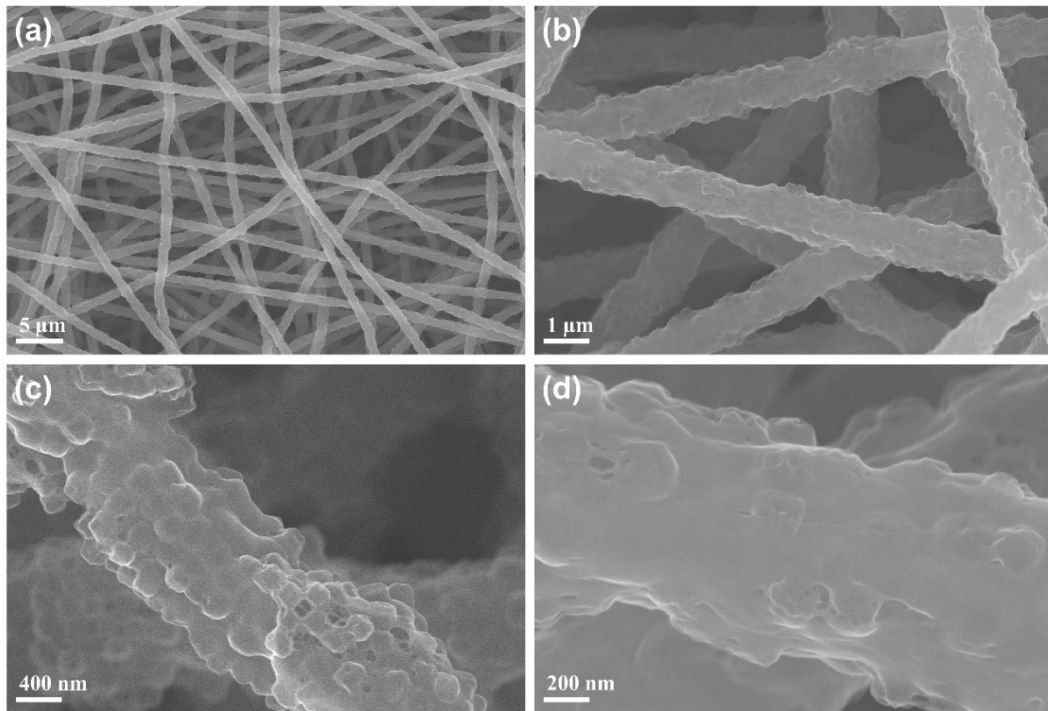


Figure S6. The SEM images of PCNFs.

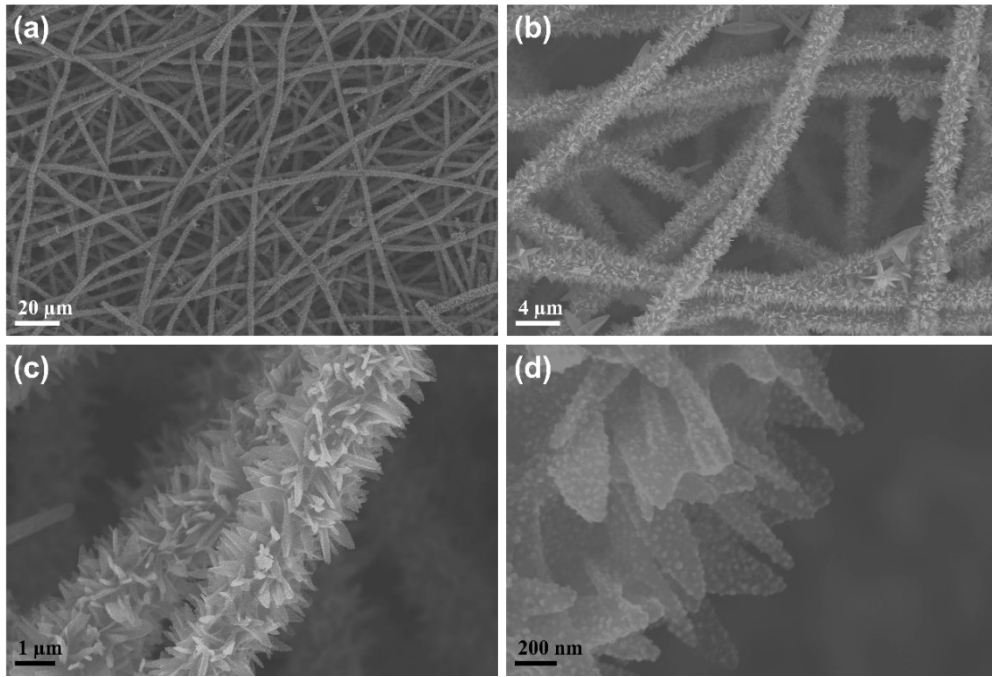


Figure S7. The SEM images of Co/PCNFs.

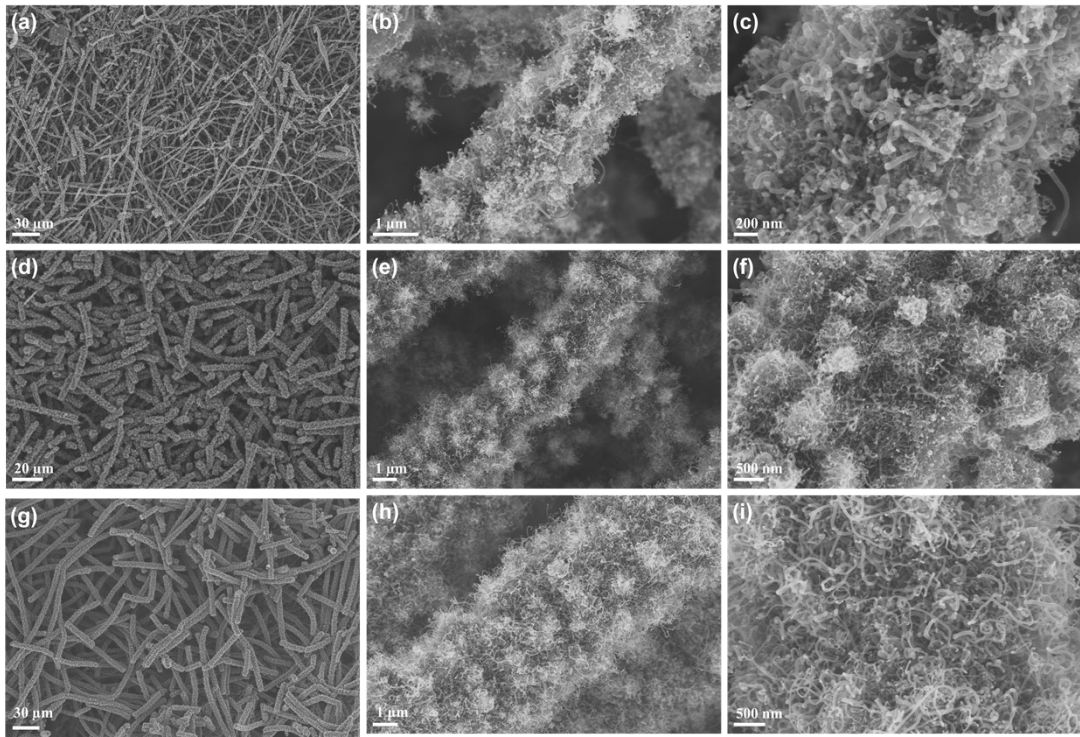


Figure S8. The SEM images of (a-c) CoCNTs/PCNFs-600 (d-f) CoCNTs/PCNFs-700 and (g-i) CoCNTs/PCNFs-900.

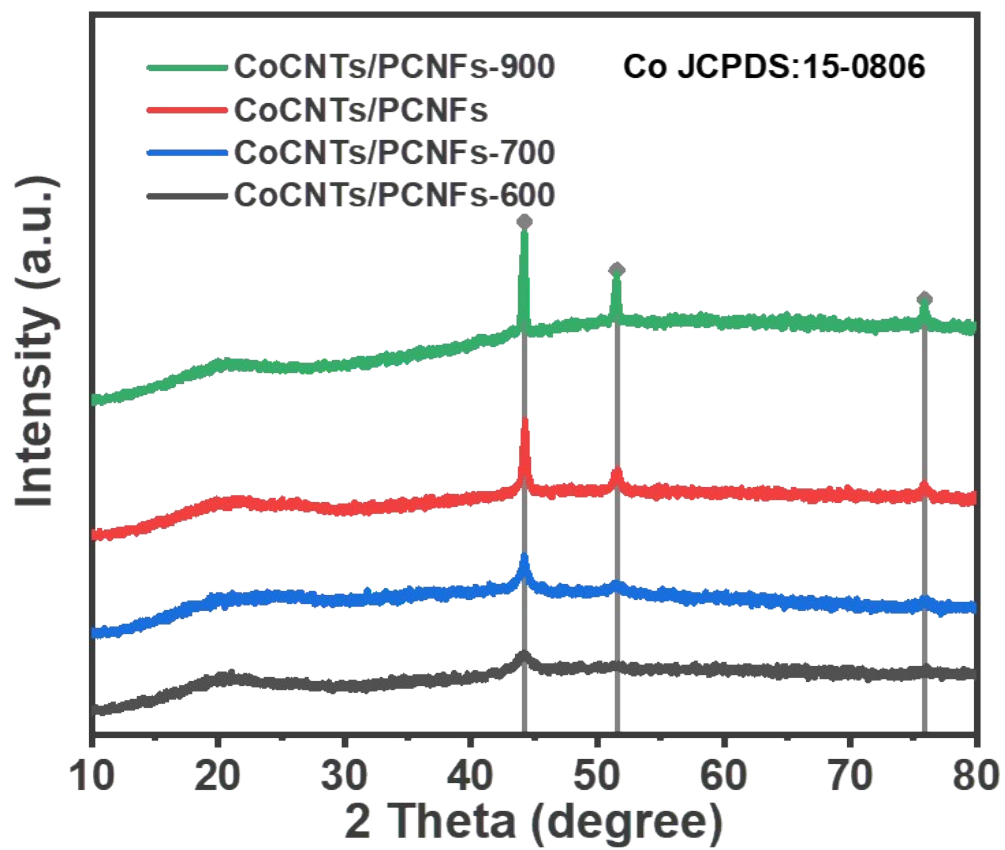


Figure S9. The XRD patterns of CoCNTs/PCNFs-*T*.

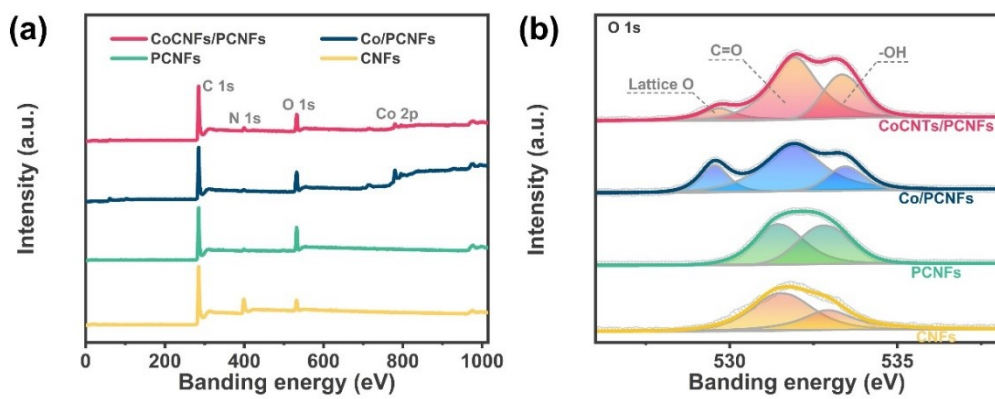


Figure S10. (a) XPS survey spectrum and (b) the deconvoluted XPS spectra of O 1s of CNFs, PCNFs, Co/PCNFs, and CoCNTs/PCNFs.

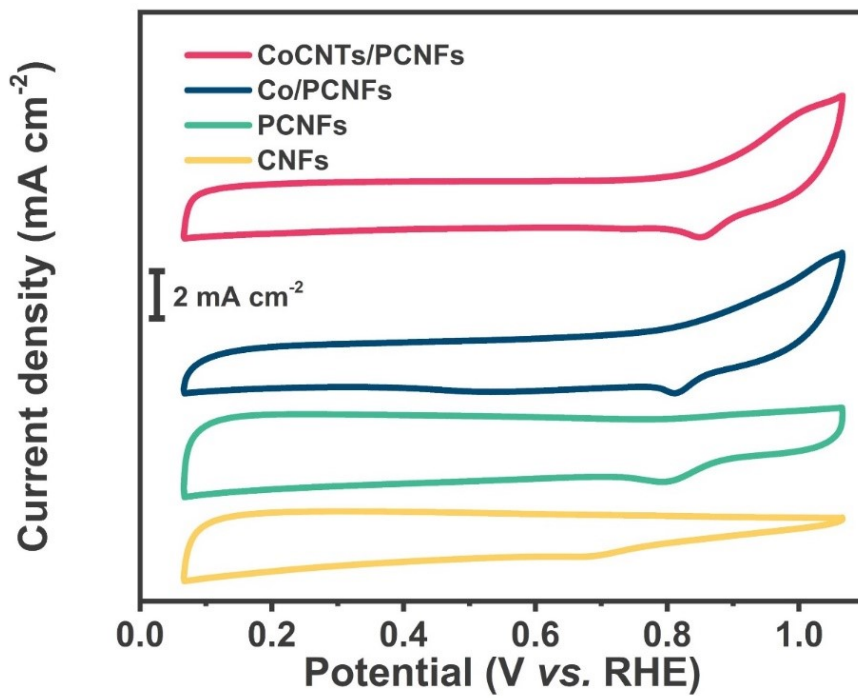


Figure S11. The CV curves of the different catalysts.

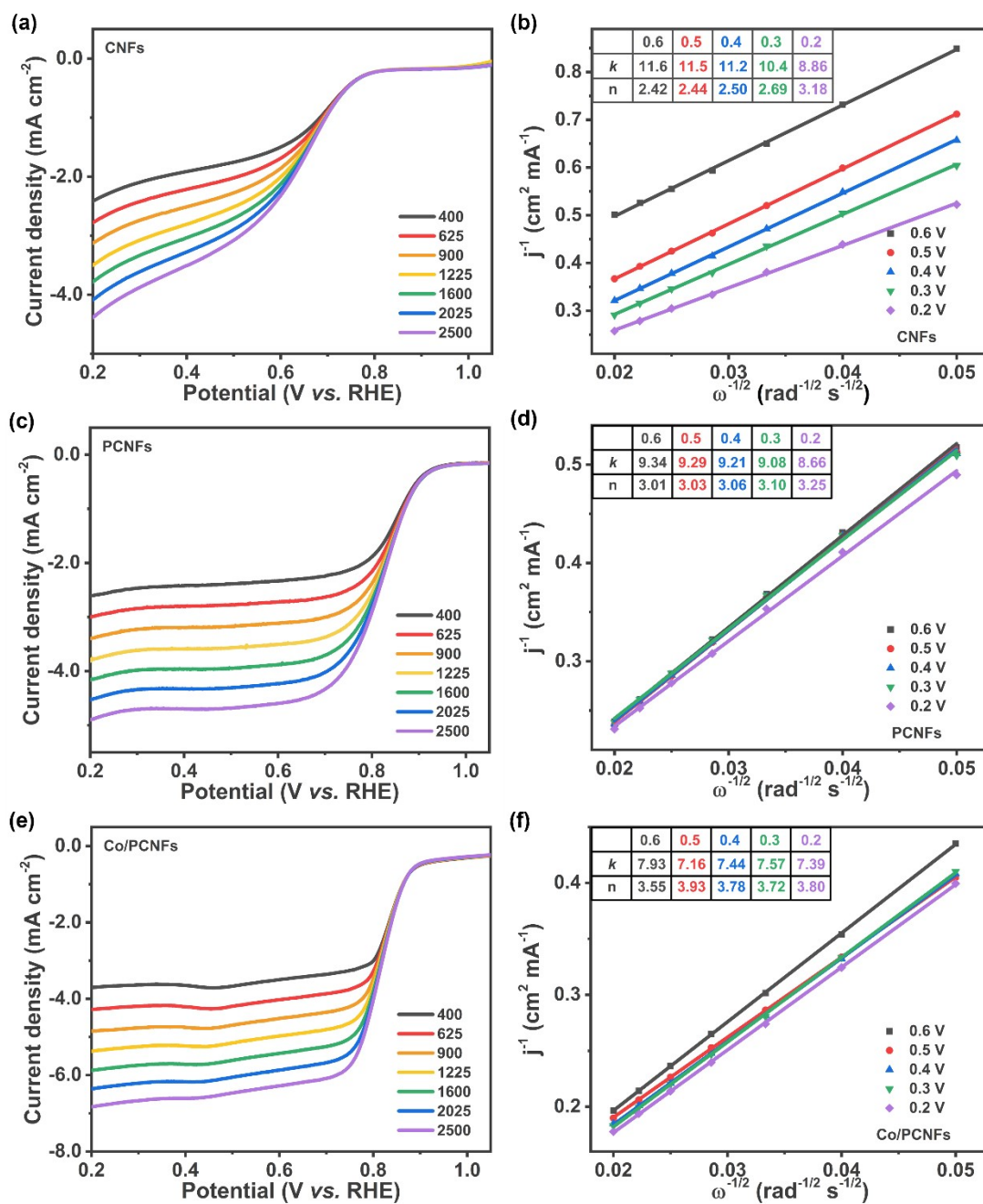


Figure S12. LSV curves and K–L plots of (a-b) CNFs, (c-d) PCNFs, and (e-f) Co/PCNFs. In the table of the figure, k is the slope of the line and n is the electron transfer number calculated by the K-L equation.

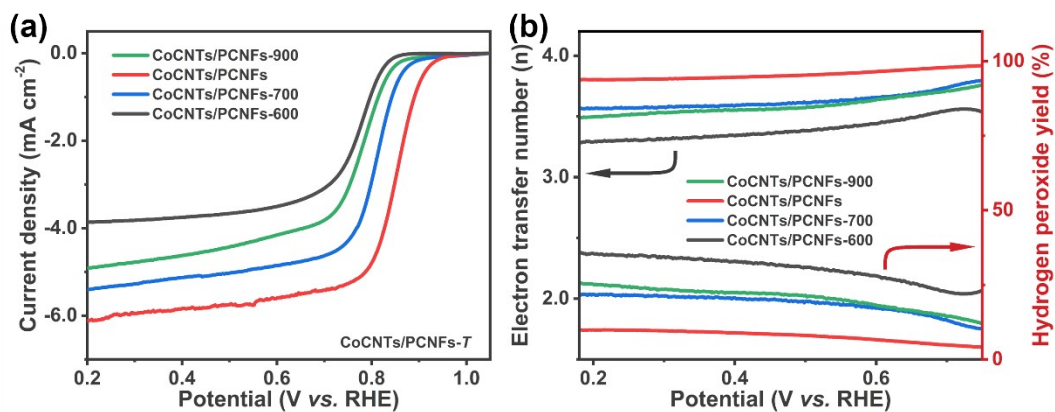


Figure S13. (a) The LSV. (b) the electron transfer number (n) and the peroxide yield (ν_{peroxide}) of CoCNTs/PCNFs- T .

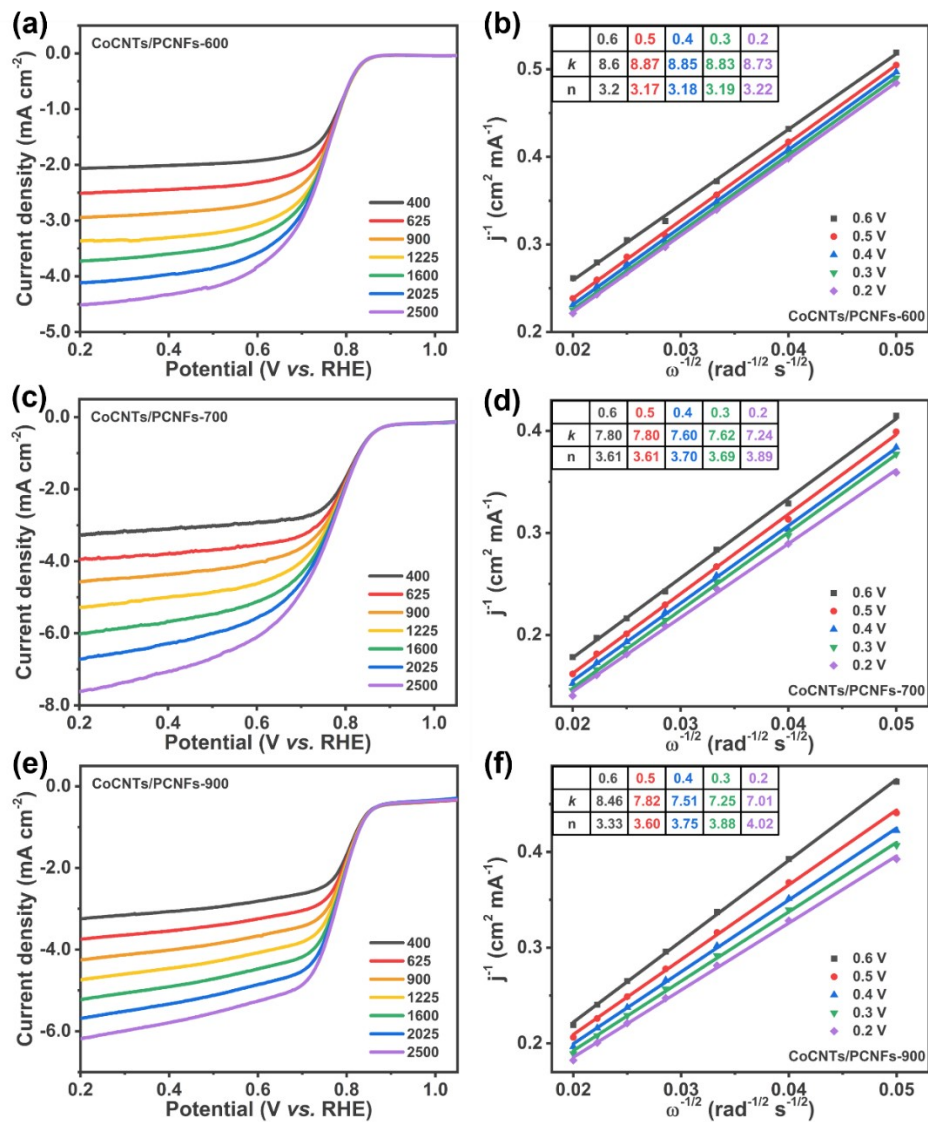


Figure S14. LSV curves and K–L plots of (a-b) CoCNTs/PCNFs-600, (c-d) CoCNTs/PCNFs-700, and (e-f) CoCNTs/PCNFs-900. In the table of the figure, k is the slope of the line and n is the electron transfer number calculated by the K-L equation.

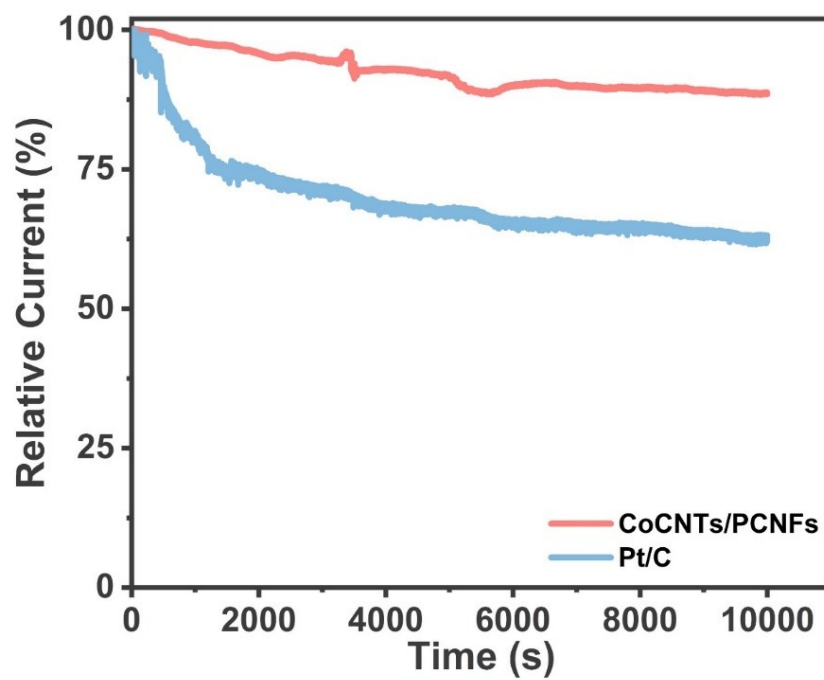


Figure S15. The ORR stability of CoCNTs/PCNFs and Pt/C.

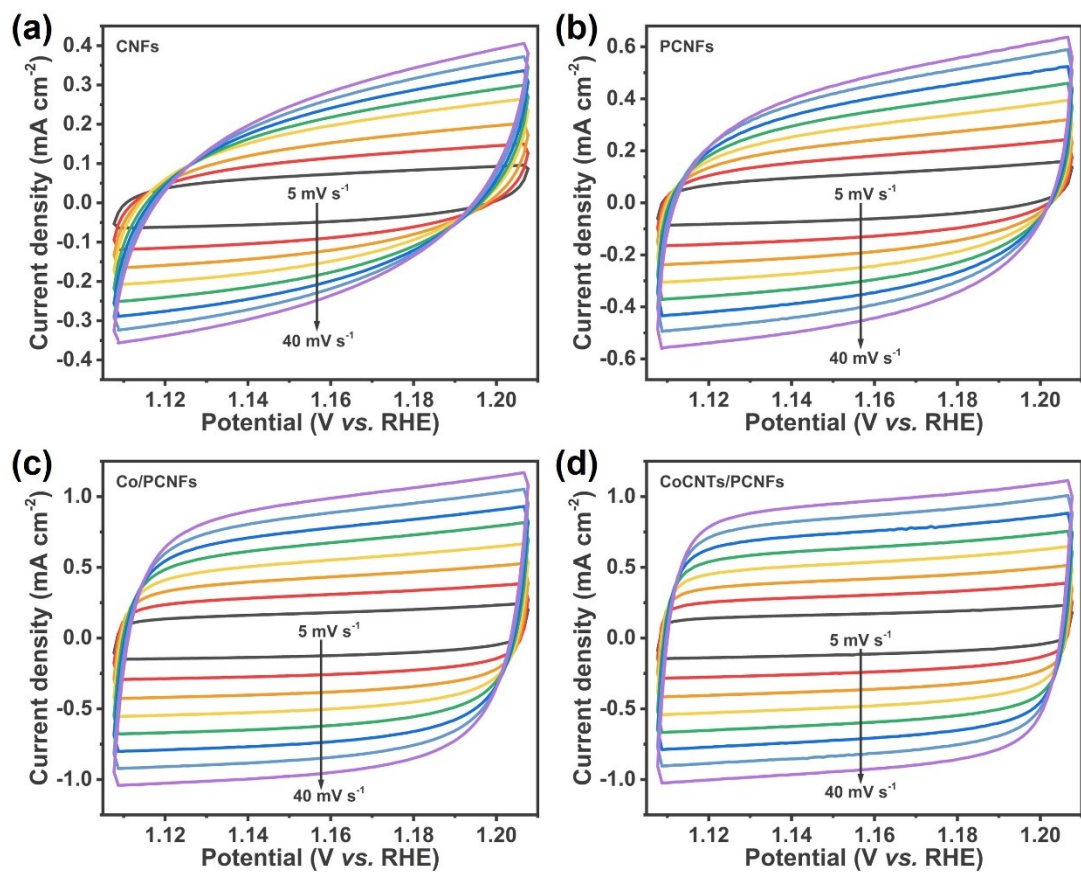


Figure S16. (a-d) The CV curves and plots of ΔJ versus scan rate of the catalysts at various scan rates.

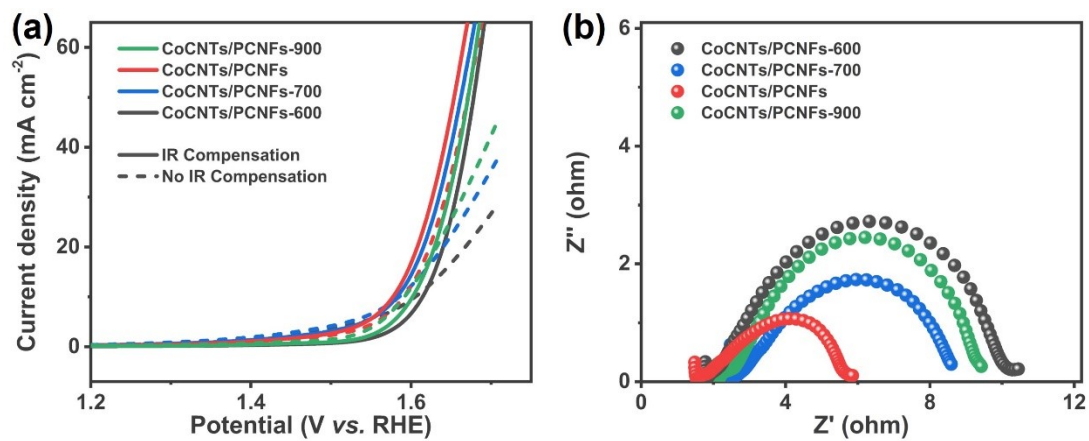


Figure S17. (a) The LSV curve of CoCNTs/PCNFs-*T* before and after IR compensation. (b) Nyquist plots of EIS spectra of CoCNTs/PCNFs-*T*.

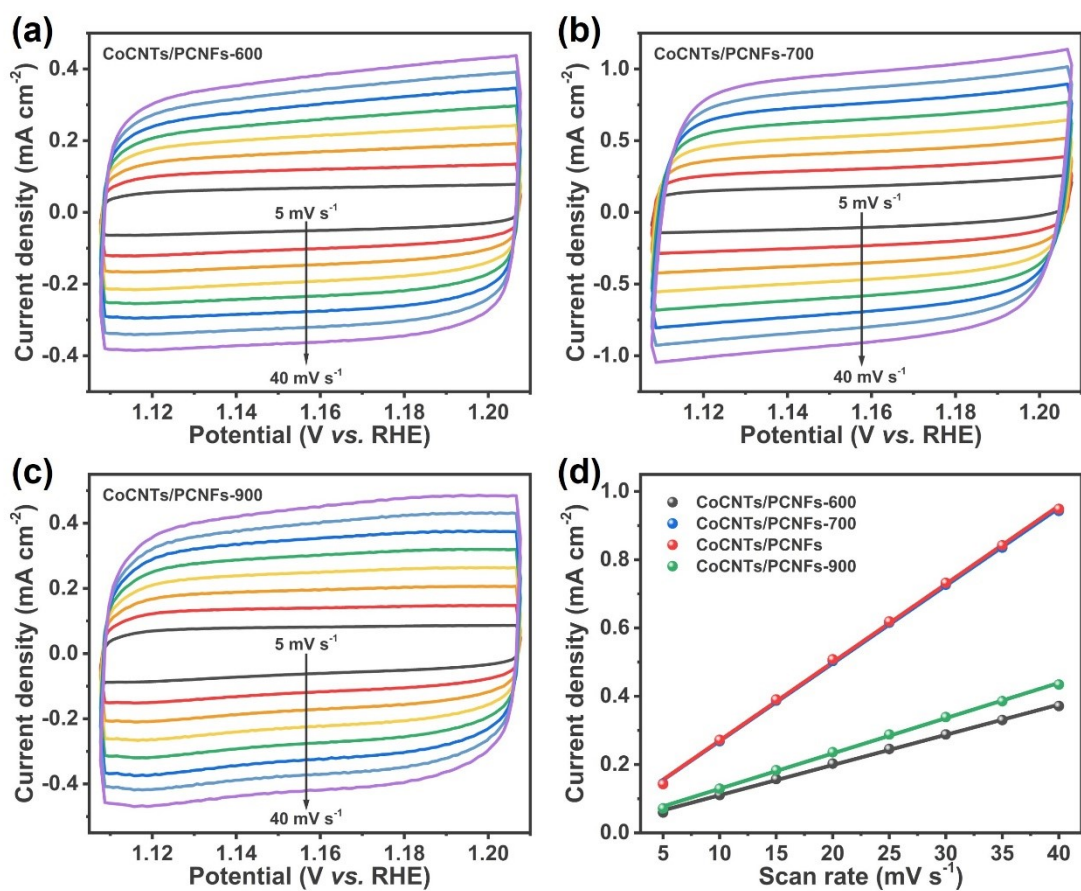


Figure S18. (a-c) The CV curves and (d) plots of ΔJ versus scan rate of the catalyst at various scan rates.

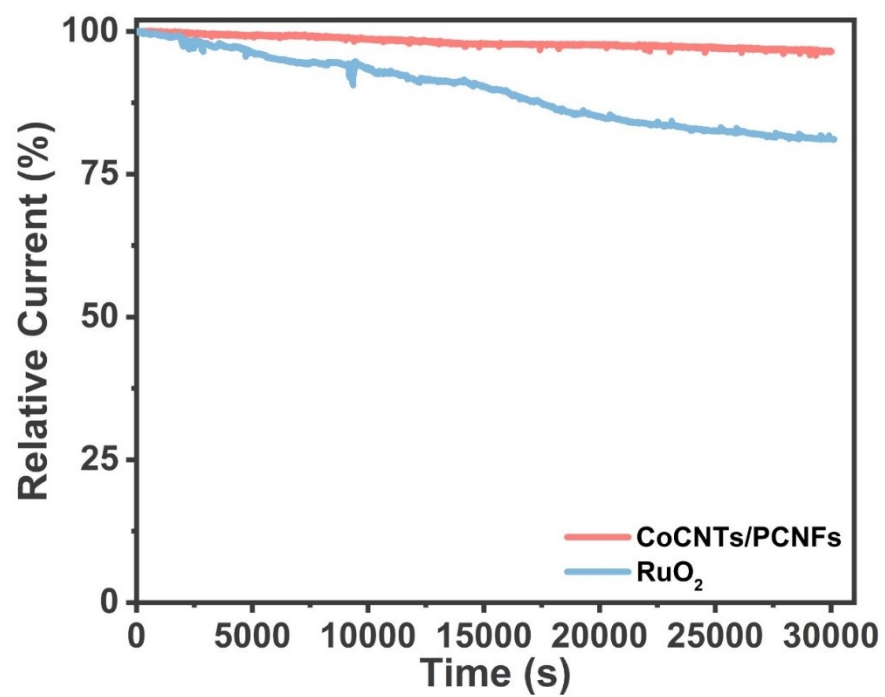


Figure S19. The stability of CoCNTs/PCNFs and RuO₂.

Table S1. List of the ORR/OER catalytic properties in alkaline solution of the CoCNTs/PCNFs and previously reported state-of-the-art catalysts.

Catalysts	ORR			OER			$\Delta E =$	Ref.	
	Electrolyte	E_{onset} (V)	$E_{1/2}$ (V)	J_{limit} (mA cm^{-2})	Electrolyte	E_{onset} (V)	$E_{(j=10)}$ (V)		$E_{(j=10)}$ $-E_{1/2}$ (V)
CoCNTs/PCNFs	0.1 M KOH	0.92	0.85	6	0.1 M KOH	1.37	1.56	0.71	This work
CoNCNTF/CNF	0.1 M KOH	0.974	0.857	5.5	0.1 M KOH	-	1.61	0.76	4
M SA@NCF/CNF	0.1 M KOH	-	0.88	-	0.1 M KOH	-	1.63	0.75	5
HoNPs@HPNCS-60	0.1 M KOH	-	0.834	-	0.1 M KOH	-	1.573	0.74	6
NiCoP/CNF900	0.1 M KOH	0.92	0.82	7.16	0.1 M KOH	1.43	1.498	0.678	7
N, P-HCNF-8	0.1 M KOH	0.93	0.82	5.1	0.1 M KOH	-	1.55	0.73	8
NiS ₂ /CoS ₂ -O NWS	0.1 M KOH	0.85	0.7	4.7	0.1 M KOH	1.46	1.5	0.8	9
Co/Co-N-C	0.1 M KOH	0.86	0.78	4.6	0.1 M KOH	-	1.54	0.76	10
FeCo-Co/CNF	0.1 M KOH	0.93	0.808	4.94	0.1 M KOH	-	1.58	0.772	11
Co ₃ O _{4-x} @N-C-2	0.1 M KOH	0.936	0.845	4.51	0.1 M KOH	-	1.75	0.905	12
Co@CNTs (1:1)	0.1 M KOH	-	0.9	6	0.1 M KOH	-	1.57	0.67	13
CoNCF-1000-80	0.1 M KOH	0.92	0.83	5.03	0.1 M KOH	1.63	1.66	0.84	14
Co-N-GCl	0.1 M KOH	0.92	0.857	5.5	0.1 M KOH	1.61	1.657	0.807	15
Co@CNT/MSiC	0.1 M KOH	0.89	0.81	4.7	0.1 M KOH	-	1.777	0.967	16
Co@NC-0.86	0.1 M KOH	0.9	0.8	4.86	0.1 M KOH	-	1.82	0.93	17
CoZn-NCNTs	0.1 M KOH	0.94	0.82	5	0.1 M KOH	-	1.83	1.01	18
Fe-N-CNFs-800	0.1 M KOH	0.98	0.86	5.12	0.1 M KOH	-	-	-	19
NiCoFe@N-CNFs	0.1 M KOH	-	0.81	4.4	0.1 M KOH	-	1.5	0.69	20
CoO-Co/CNF	0.1 M KOH	0.95	0.858	2.9	0.1 M KOH	-	1.667	0.809	21
NCNF-1000	0.1 M KOH	0.97	0.8	4.7	0.1 M KOH	1.43	1.84	1.02	22
Co@CNFs-50-800	0.1 M KOH	0.88	0.8	5	0.1 M KOH	1.50	1.54	0.74	23
H-NSC@Co/NSC	0.1 M KOH	0.98	0.85	5.6	0.1 M KOH	1.5	1.6	0.75	24

Table S2. A comparison of Zn-Air battery performances of this work with reported catalysts.

Catalysts	Electrolytes	Open-circuit voltage (V)	cycle life (h)	Capacity (mAh/g ⁻¹)	Power density (mW/cm ²)	Ref.
CoCNTs/PCNFs	6 M KOH + 0.2 M Zn(OAc)₂	1.455	100	760	262.6	This work
Co@CNTs	6 M KOH + 0.2 M ZnCl ₂	-	40	-	149.2	25
Co@NC-0.86	6 M KOH + 0.2 M Zn(OAc) ₂	1.386	-	663	95	26
CoZn-NCNTs	6 M KOH	1.46	92	757	214	27
Fe/3S/N-C	6 M KOH	1.5	-	672	94	28
Fe-N-CNTs-800	6 M KOH	1.5	-	614	-	29
SAFe-SWCNT	6 M KOH + 0.2 M Zn(OAc) ₂	1.47	33	772	210	30
Co-N _x /C NRA	6 M KOH + 0.2 M Zn(OAc) ₂	1.42	80	-	193.2	31
Fe@C-NG/NCNT	6 M KOH + 0.2 M Zn(OAc) ₂	1.44	99	682	146.5	32
Co-Ni@NSPC	6 M KOH + 0.2 M Zn(OAc) ₂	1.54	60	-	51.6	33
(Co, Mg)S ₂ @CNT	6 M KOH	1.4	50	-	268	34
CoIn ₂ S ₄ /S-rGO	6 M KOH + 0.2 M ZnCl ₂	1.42	50	745	133	35
NiFe/NCNF/CC	6 M KOH + 0.2 M Zn(OAc) ₂	-	20	730	140.1	36
Ni ₃ Fe/N-C sheets	6 M KOH + 0.2 M ZnCl ₂	-	-	528	-	37
CoN _x /Zn-NC	6 M KOH + 0.2 M Zn(OAc) ₂	1.48	115	718.9	164.1	38
Co@CNFs-50-800	6 M KOH + 0.2 M Zn(OAc) ₂	1.46	160	809	165.5	23
H-NSC@Co/NSC	6 M KOH + 0.2 M Zn(OAc) ₂	1.512	-	828	204.3	24

References

- 1 X. Hu, G. Zhong, J. Li, Y. Liu, J. Yuan, J. Chen, H. Zhan and Z. Wen, Hierarchical porous carbon nanofibers for compatible anode and cathode of potassium-ion hybrid capacitor, *Energy Environ. Sci.*, 2020, **13**, 2431-2440.
- 2 M. Li, Q. Yang, L. Fan, X. Dai, Z. Kang, R. Wang and D. Sun, An Ultrastable Bifunctional Electrocatalyst Derived from a Co²⁺-Anchored Covalent-Organic Framework for High-Efficiency ORR/OER and Rechargeable Zinc-Air Battery, *ACS Appl. Mater. Interfaces*, 2023, **15**, 39448-39460.
- 3 L. Zheng, S. Yu, X. Lu, W. Fan, B. Chi, Y. Ye, X. Shi, J. Zeng, X. Li and S. Liao, Two-Dimensional Bimetallic Zn/Fe-Metal-Organic Framework (MOF)-Derived Porous Carbon Nanosheets with a High Density of Single/Paired Fe Atoms as High-Performance Oxygen Reduction Catalysts, *ACS Appl. Mater. Interfaces*, 2020, **12**, 13878-13887.
- 4 D. Ji, L. Fan, L. Li, N. Mao, X. Qin, S. Peng and S. Ramakrishna, Hierarchical catalytic electrodes of cobalt-embedded carbon nanotube/carbon flakes arrays for flexible solid-state zinc-air batteries, *Carbon*, 2019, **142**, 379-387.
- 5 D. Ji, L. Fan, L. Li, S. Peng, D. Yu, J. Song, S. Ramakrishna and S. Guo, Atomically transition metals on self-supported porous carbon flake arrays as binder-free air cathode for wearable zinc-air batteries, *Adv. Mater.*, 2019, **31**, 1808267.
- 6 D. Ji, L. Fan, L. Tao, Y. Sun, M. Li, G. Yang, T. Q. Tran, S. Ramakrishna and S. Guo, The kirkendall effect for engineering oxygen vacancy of hollow Co₃O₄ nanoparticles toward high-performance portable zinc-air batteries, *Angew. Chem. Int. Ed.*, 2019, **58**, 13840-13844.
- 7 S. Surendran, S. Shanmugapriya, A. Sivanantham, S. Shanmugam and R. K. Selvan, Electrospun carbon nanofibers encapsulated with NiCoP: a multifunctional electrode for supercapattery and oxygen reduction, oxygen evolution, and hydrogen evolution reactions, *Adv. Energy Mater.*, 2018, **8**, 1800555.
- 8 Y. Gao, Z. C. Xiao, D. B. Kong, R. Iqbal, Q. H. Yang and L. J. Zhi, N, P co-doped hollow carbon nanofiber membranes with superior mass transfer property for

- trifunctional metal-free electrocatalysis, *Nano Energy*, 2019, **64**, 103879.
- 9 J. Yin, Y. Li, F. Lv, M. Lu, K. Sun, W. Wang, L. Wang, F. Cheng, Y. Li, P. Xi and S. Guo, Oxygen vacancies dominated NiS₂/CoS₂ interface porous nanowires for portable Zn-air batteries driven water splitting devices, *Adv. Mater.*, 2017, **29**, 1704681.
- 10 P. Yu, L. Wang, F. Sun, Y. Xie, X. Liu, J. Ma, X. Wang, C. Tian, J. Li and H. Fu, Co Nanoislands rooted on Co-N-C nanosheets as efficient oxygen electrocatalyst for Zn-air batteries, *Adv. Mater.*, 2019, **31**, 1901666.
- 11 X. Liu, S. Peng, X. Li, C. Liu, J. Zeng, X. Qi and T. Liang, Encapsulation of FeCo-Co nanoparticles in N-Doped carbon nanotubes as bifunctional catalysts for Zn-air battery, *J. Electrochem. Soc.*, 2021, **168**, 090514.
- 12 Y. Wang, R. Gan, Z. Ai, H. Liu, C. Wei, Y. Song, M. Dirican, X. Zhang, C. Ma and J. Shi, Hollow Co₃O_{4-x} nanoparticles decorated N-doped porous carbon prepared by one-step pyrolysis as an efficient ORR electrocatalyst for rechargeable Zn-air batteries, *Carbon*, 2021, **181**, 87.
- 13 J. Jiao, Y. Pan, B. Wang, W. Yang, S. Liu and C. Zhang, Melamine-assisted pyrolytic synthesis of bifunctional cobalt-based core-shell electrocatalysts for rechargeable zinc-air batteries, *J. Energy Chem.*, 2021, **53**, 364.
- 14 H. Jiang, Y. Liu, W. Li and J. Li, Co Nanoparticles Confined in 3D Nitrogen-Doped Porous Carbon Foams as Bifunctional Electrocatalysts for Long-Life Rechargeable Zn-Air Batteries, *Small*, 2018, **14**, 1703739.
- 15 X. Qiao, S. Liao, R. Zheng, Y. Deng, H. Song and L. Du, Cobalt and nitrogen codoped graphene with inserted carbon nanospheres as an efficient bifunctional electrocatalyst for oxygen reduction and evolution, *ACS Sustain. Chem. Eng.*, 2016, **4**, 4131.
- 16 C. Xiao, J. Luo, M. Tan, Y. Xiao, B. Gao, Y. Zheng and B. Lin, Co/CoN_x decorated nitrogen-doped porous carbon derived from melamine sponge as highly active oxygen electrocatalysts for zinc-air batteries, *J. Power Sources*, 2020, **453**, 227900.

- 17 R. Zhang, A. Ma, X. Liang, L. Zhao, H. Zhao and Z. Yuan, Cobalt nanoparticle decorated N-doped carbons derived from a cobalt covalent organic framework for oxygen electrochemistry, *Front. Chem. Sci. Eng.*, 2021, **15**, 1550.
- 18 X. Liu, L. Wang, G. Zhang, F. Sun, G. Xing, C. Tian and H. Fu, Zinc assisted epitaxial growth of N-doped CNTs-based zeolitic imidazole frameworks derivative for high efficient oxygen reduction reaction in Zn-air battery, *Chem. Eng. J.*, 2021, **414**, 127569.
- 19 Z. Wu, X. Xu, B. Hu, H. Liang, Y. Lin, L. Chen and S. Yu, Iron carbide nanoparticles encapsulated in mesoporous Fe-N-doped carbon nanofibers for efficient electrocatalysis, *Angew. Chem. Int. Ed.*, 2015, **54**, 8179.
- 20 F. Cao, X. Yang, C. Shen, X. Li, J. M. Wang, G. W. Qin, S. Li, X. Y. Pang and G. Q. Li, Electrospinning synthesis of transition metal alloy nanoparticles encapsulated in nitrogen-doped carbon layers as an advanced bifunctional oxygen electrode, *J. Mater. Chem. A*, 2020, **8**, 7245-7252.
- 21 C. Alegre, C. Busacca, O. Di Blasi, V. Antonucci, A. S. Arico, A. Di Blasi and V. Baglio, A combination of CoO and Co nanoparticles supported on electrospun carbon nanofibers as highly stable air electrodes, *J. Power Sources*, 2017, **364**, 101-109.
- 22 Q. Liu, Y. Wang, L. Dai and J. Yao, Scalable fabrication of nanoporous carbon fiber films as bifunctional catalytic electrodes for flexible Zn-air batteries, *Adv. Mater.*, 2016, **28**, 3000-3006.
- 23 X. Yin, Q. Liu, Y. Ding, K. Chen, P. Cai and Z. Wen, Hierarchical Carbon/Metal Nanostructure with a Combination of 0D Nanoparticles, 1D Nanofibers, and 2D Nanosheets: An Efficient Bifunctional Catalyst for Zinc-Air Batteries, *ChemElectroChem*, 2021, **8**, 1107-1116.
- 24 W. Li, J. Wang, J. Chen, K. Chen, Z. Wen and A. Huang, Core-Shell Carbon-Based Bifunctional Electrocatalysts Derived from COF@MOF Hybrid for Advanced Rechargeable Zn-Air Batteries, *Small*, 2022, **18**, 2202018.
- 25 J. Jiao, Y. Pan, B. Wang, W. Yang, S. Liu and C. Zhang, Melamine-assisted pyrolytic synthesis of bifunctional cobalt-based core-shell electrocatalysts for

- rechargeable zinc-air batteries, *J. Energy Chem.*, 2021, **53**, 364.
- 26 R. Zhang, A. Ma, X. Liang, L. Zhao, H. Zhao and Z. Yuan, Cobalt nanoparticle decorated N-doped carbons derived from a cobalt covalent organic framework for oxygen electrochemistry, *Front. Chem. Sci. Eng.*, 2021, **15**, 1550.
- 27 X. Liu, L. Wang, G. Zhang, F. Sun, G. Xing, C. Tian and H. Fu, Zinc assisted epitaxial growth of N-doped CNTs-based zeolitic imidazole frameworks derivative for high efficient oxygen reduction reaction in Zn-air battery, *Chem. Eng. J.*, 2021, **414**, 127569.
- 28 Z. Xiao, Y. Wu, S. Cao, W. Yan, B. Chen, T. Xing, Z. Li, X. Lu, Y. Chen, K. Wang and J. Jiang, An active site pre-anchoring and post-exposure strategy in $\text{Fe}(\text{CN})_6^{4-}$ @PPy derived Fe/S/N-doped carbon electrocatalyst for high performance oxygen reduction reaction and zinc-air batteries, *Chem. Eng. J.*, 2021, **413**, 127395.
- 29 Z. Wu, X. Xu, B. Hu, H. Liang, Y. Lin, L. Chen and S. Yu, Iron carbide nanoparticles encapsulated in mesoporous Fe-N-doped carbon nanofibers for efficient electrocatalysis, *Angew. Chem. Int. Ed.*, 2015, **54**, 8179.
- 30 Y. Meng, J. Li, S. Zhao, C. Shi, X. Li, L. Zhang, P. Hou, C. Liu and H. Cheng, Fluorination-assisted preparation of self-supporting single-atom Fe-N-doped single-wall carbon nanotube film as bifunctional oxygen electrode for rechargeable Zn-Air batteries, *Appl. Catal. B*, 2021, **294**, 120239.
- 31 I. S. Amiin, X. Liu, Z. Pu, W. Li, Q. Li, J. Zhang, H. Tang, H. Zhang and S. Mu, From 3D ZIF nanocrystals to $\text{Co-N}_x/\text{C}$ nanorod array electrocatalysts for ORR, OER, and Zn-air batteries, *Adv. Funct. Mater.*, 2018, **28**, 1704638.
- 32 Q. Wang, Y. Lei, Z. Chen, N. Wu, Y. Wang, B. Wang and Y. Wang, $\text{Fe}/\text{Fe}_3\text{C}@C$ nanoparticles encapsulated in N-doped graphene-CNTs framework as an efficient bifunctional oxygen electrocatalyst for robust rechargeable Zn-air batteries, *J. Mater. Chem. A*, 2018, **6**, 516.
- 33 W. Fang, H. Hu, T. Jiang, G. Li and M. Wu, N- and S-doped porous carbon decorated with in-situ synthesized Co-Ni bimetallic sulfides particles: a cathode catalyst of rechargeable Zn-air batteries, *Carbon*, 2019, **146**, 476-485.

- 34 J. Guo, N. Xu, Y. Wang, X. Wang, H. Huang and J. Qiao, Bimetallic sulfide with controllable mg substitution anchored on CNTs as hierarchical bifunctional catalyst toward oxygen catalytic reactions for rechargeable zinc-air batteries, *ACS Appl. Mater. Interfaces*, 2020, **12**, 37164-72.
- 35 G. Fu, J. Wang, Y. Chen, Y. Liu, Y. Tang, J. B. Goodenough and J. M. Lee, Exploring indium-based ternary thiospinel as conceivable high-potential air-cathode for rechargeable Zn-Air batteries, *Adv. Energy Mater.*, 2018, **8**, 1802263.
- 36 C. Lai, J. Fang, X. Liu, M. Gong, T. Zhao, T. Shen, K. Wang, K. Jiang and D. Wang, In situ coupling of NiFe nanoparticles with N-doped carbon nanofibers for Zn-air batteries driven water splitting, *Appl. Catal. B*, 2021, **285**, 119856.
- 37 G. Fu, Z. Cui, Y. Chen, Y. Li, Y. Tang and J. B. Goodenough, Ni₃Fe-N doped carbon sheets as a bifunctional electrocatalyst for air cathodes, *Adv. Energy Mater.*, 2017, **7**, 1601172.
- 38 L. Xu, D. Deng, Y. Tian, H. Li, J. Qian, J. Wu and H. Lia, Dual-active-sites design of CoN_x anchored on zinc-coordinated nitrogen-codoped porous carbon with efficient oxygen catalysis for high-stable rechargeable zinc-air batteries, *Chem. Eng. J.*, 2021, **408**, 127321.